

## Fabrication Co-TiO<sub>2</sub> Nanoparticles by TCVD for Water Treatment and Desalination

Roya.Bakhshkandi<sup>1</sup>, Sosun.Zoriatain<sup>2</sup>, Mohammad.Samipoor Giri<sup>3\*</sup>,  
Mostafa.Sefidgar<sup>4</sup>

<sup>1,2</sup>*Physics Department, Islamic Azad University, North Tehran Branch, Tehran, Iran*

<sup>3</sup>*Chemical Engineering Department, Islamic Azad University, North Tehran Branch, Tehran, Iran*

<sup>4</sup>*Mechanical Engineering Department, Islamic Azad University, Pardis Branch, Tehran, Iran*

### Abstract

*Synthesis of titanium dioxide nanoparticles using TTIP and TTIP+EtOH precursor at 600°C through chemical precipitation of vapours by heat is studied. Precursor and feed gas (Ar+NH<sub>3</sub>/Ar) concentration effects, the effect of catalyst on particle growth, thickness and surface roughness on the size and numbers of particles, crystallinity, phase transition and nanoparticles purity are studied using elemental analysis techniques such as EDX, FESEM, AFM and RBS. The results indicate a growth in particle size due to concentration variations in the precursors and addition of ethanol in a manner that allows for the control of nanoparticles initial size through adjustment of these parameters. The results further indicated that ethanol causes a significant increase on particle size and growth. The addition of ammonia to feed gas resulted in a reduction of particle size and titanium dioxide nanoparticles which have applications in desalination and purification of seawater due to their photocatalytic effect, were used to increase the efficiency of RO systems.*

**Keywords:** Nexus, titanium dioxide, thermal chemical vapor deposition, TTIP, photocatalytic

### 1. Introduction

Nexus conveys the interactions between two elements, be they dependencies or interdependencies. Water is not only needed in the energy supply chain, but energy is also needed to extract, dispense and treat water. The water sector uses energy, to a large extent, in the form of electricity [1].

Water is necessary for life and water pollution is a major challenge for the environment. Exposure to toxic organic chemicals, dyes and pharmaceutical drugs even in trace amounts can have long term implication on every kind of life. Photocatalytic degradation has emerged as an efficient technique to eliminate such water pollutants[2-5].

For efficient accommodation of such new construction materials, the nanosized component should be fundamentally studied in order to address its complementarity and performance[6-8]. The rapidly growing world population over the past few decades has created a huge demand for resource supplies, especially fresh water resources [9,10]. Among the various methods to obtain accessible water, membrane technology shines in many industrial fields including food, medicine, water purification and wastewater treatment due to its distinct advantages [11–14]. However, membrane fouling leads to significantly increased cost which is known as the predominant obstacle for membrane industry [15–17]. The inherent hydrophobicity of organic membranes makes it easier to be adhered by natural organic matters, causing fouling difficulty [18–20]. Membrane fouling generally occurs in the primary fouling mechanisms of pore blocking, foulant

---

\* Corresponding Author

adhesion and osmotic pressure effects during foulant layer filtration [21–23]. Improving membrane surface hydrophilicity is believed to be efficient to mitigate membrane fouling [24–26]. Therefore, hydrophilic modification of polymeric membranes is attracting more and more attention, and becomes one of the hottest topics in separation membrane field [27–29]. Addition of hydrophilic materials can reduce hydrophobicity of membrane and is playing an important role in promoting antifouling ability of polymeric membranes.

Photocatalytic cement-based materials are a relatively new group of smart materials produced by addition of photo-activated heterogeneous semiconductors in the form of nanoparticles [6-8]. The added hydrophilic materials including organic poly vinylpyrrolidone[30,31], chitosan [32], polyethylene glycol[33] and inorganic nanoparticles such as titanium dioxide [34], silicon dioxide [35], zinc oxide [36], carbon nanotubes [37], iron oxide [38], silver [39], etc., have been reported. Titanium dioxide in anatase form is almost without exception, the most featured and widely used semiconductor for commercial photocatalytic applications [40]. The photocatalytic performance of titania has been found to be even more efficient if the semiconductor is in nanoparticle form [41], due to its high specific surface area to volume ratio, which enables improvements in catalysis.

Among these mentioned hydrophilic matters, titanium dioxide ( $\text{TiO}_2$ ) possesses the particular attractions due to its inexpensive cost, non-toxic property, good chemical stability and photocatalytic property [42,43]. Researchers have found that titanium dioxide in polymer matrix can not only improve the hydrophilicity, but also endow the membranes with a certain extent self-cleaning ability [44,45]. In spite of this, the positive effects of titanium dioxide have been seriously limited because the titanium dioxide particles with relative higher density always settle to the bottom of the polymeric membrane bulk during the phase transition process [46]. Therefore, there is a great desire to anchor the titanium dioxide particles onto the membrane surface so that the titanium dioxide particles can sufficiently demonstrate their advantages. Recently, magnetic nanoparticles(NPs) have received increasing attention in the environmental field due to magnetic recycling and some additional properties. Some studies reported that the surface of membrane fixed by nanoparticles in an external force (electric field or magnetic field) presented certain hydrophilicity and pollution resistance to the membrane [47,48]. For instance, Huang et al. [49] proved that the  $\text{Fe}_3\text{O}_4/\text{GO}/\text{PVDF}$  membrane prepared by magnetic field induction possessed an excellent permeation flux and pollution resistance. This concept may be introduced to concentrate the magnetic titanium dioxide nanoparticles onto the membrane surface so that titanium dioxide ( $\text{TiO}_2$ ) nanoparticles can sufficiently display their antifouling and self-cleaning ability.

In summary, major contributions of this work are that highly crystalline  $\text{TiO}_2$  nanoparticles are prepared by thermal chemical vapor deposition(TCVD).

## **2. Experiment**

### **2.1. Selection of substrata**

Silicon was selected as the substrate for experiments. P (100) type silicon was selected as the substrate due to its availability and affordability as well as its favourable properties. General requirements for any substrate include:

1. Melting point above the required melting point for growth of titanium dioxide nanoparticles while using TCVD systems.
2. Comparable thermal expansion coefficient with that of titanium.

### **2.2. Substrate Preparation**

Once a suitable substrate is selected for thin film deposition, it must be prepared for the experiment. Since chemical bond forces have a limited range of a few nanometres, adhesion between the layers is weak. On the other hand, impurities may affect the photo electronic structure of the layers. Pollutants generally comprise of water and fats which have been transferred from the ambient, machinery or labour. These pollutants can often be eliminated using degreasing solvents

such as acetone and trichloroethylene. Substrates used for deposition are cleaned with acetone and distilled water using ultrasonic and then dried.

### 2.3. Cobalt catalyst deposition

After the substrate is completely cleaned from pollutants using the available methods, and is ready for deposition, a thin film of cobalt will be deposited using PECVD for deposition under vacuum conditions, where system pressure is reduced to  $2.5 \times 10^{-2}$  torr. In order to initiate deposition, argon is introduced to the reactor at the flow of 100 SCCM and deposition is performed using argon gas plasma. From here on out, depending on the deposition period, layers of cobalt with various thicknesses form and RBS analysis is used to determine their thickness, while AFM analysis is used to determine their surface roughness. Layers of 6.5 nm thickness are then used.

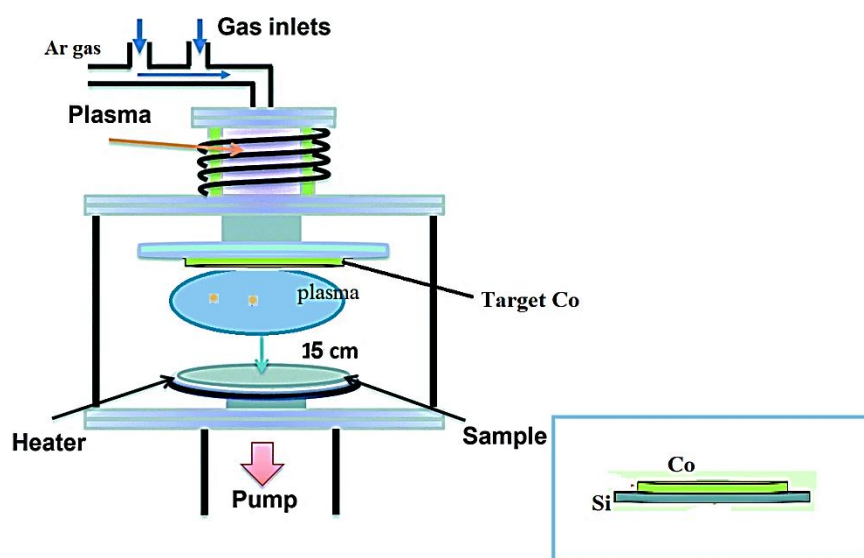


Figure1. Schematic of Plasma Deposition System

### 2.4. Etching

In order to grow, titanium dioxide nanostructures require nanometric stations on the catalyst surface which are directly dependant on the catalyst layer thickness, i.e. very thin films a few nanometres thick are not yet continuous and appear in form of islands on the substrate, several nanometres in diameter; these islands could then be used as stations to grow nanostructures. As the layer thickens, the layers become more continuous and isolated islands disappear, but since the layer surface is not completely flat, the nanometric stations will sporadically form on the surface. In order to facilitate this process, and with the aim of increasing the number of such stations, etching on the layer is performed a few minutes prior to the initiation of nanostructure growth, resulting in increased surface roughness and formation of additional nanometric stations on the surface.

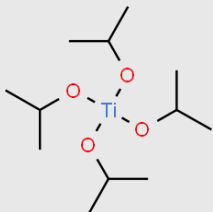
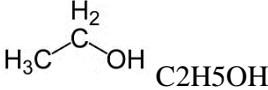
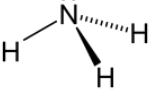
During the next stage, the cobalt catalyst covered substrate is inserted into the chamber using a TCVD device at 500 °C, with argon gas as diluent and ammonia gas with 100 SCCM flow, and etching is performed. During etching, oxidation and reduction occurs where every metal in contact with the gases shows tendency for ionization through electron release; the samples are then AFM analysed.

### 2.5. Nanoparticle Synthesis

### 2.5.1. Materials

Materials which were used in the experimental method are submitted below.

**Table 1. The Chemicals Used in the Experimental Method**

Chemical	Formula	Purity(%)
Titanium isopropoxide(TTIP)	 $Ti(OCH(CH_3)_2)_4$	97(Sigma Aldrich)
Ethanol	 $C_2H_5OH$	96(Carlo Erba)
Argon	Ar	99.99
ammonia(NH <sub>3</sub> )		99.98

Preparation of nanoparticles is performed using chemical precipitation of vapours using heat.

Various factors including solvent and catalyst type and composition, bedding type, bedding catalyst weight percent and temperature will affect the dimensions of synthesized nanoparticles whereas particle growth is influenced by factors such as growth time, growth temperature and gas flow velocities.

The effect of some of these parameters on the synthesized nanoparticles(NPs) dimensions and the consequential growth of titanium dioxide nanoparticles is studied. Titanium dioxide nanoparticle synthesis through deposition from chemical vapour phase is analysed using variations in temperature, feeding gas and precursor.

Thermal CVD was performed in an electric furnace. The furnace used pure tungsten as heating element and the reactor chamber for this setup consists of a 800 mm long quartz pipe with an internal diameter of 75 mm surrounded in a furnace with controllable set point.

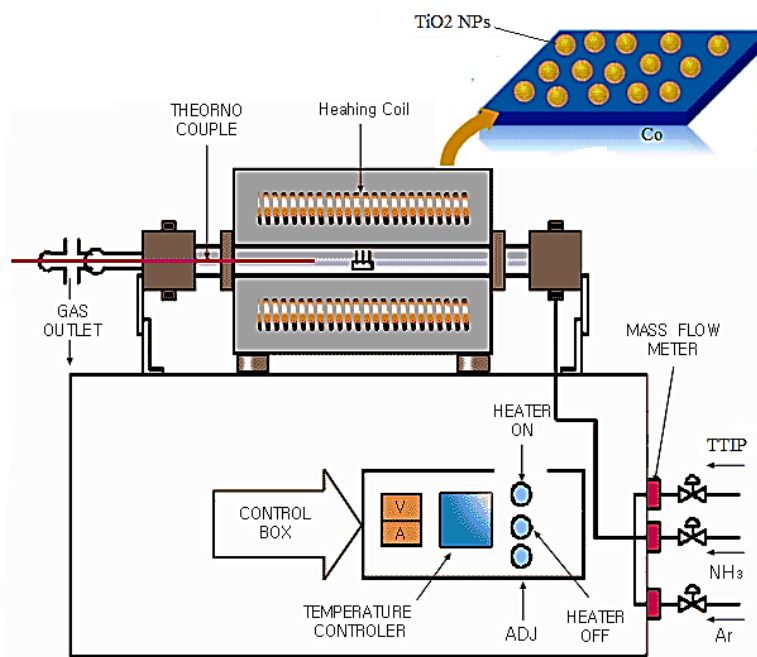


**Figure 2a. Schematic Diagram of TCVD Device**



**Figure 2b. Photographic View of TCVD Device**

In order to synthesize titanium dioxide nanoparticles, the bedding catalyst particles are prepared first and then a crucible containing the cobalt catalyst is inserted into the reactor in which the flow of feeding gas has already been established. The feeding gas which flows through the furnace consists of ammonia and argon as carrier gas.

Since argon is selected as the carrier gas due to its inertness and relatively higher weight compared with other inert gases, it best suits the transfer of hydrocarbon gases to the reaction zone and on the other hand assists the removal of unneeded reaction by-product gases, from the catalyst and the reaction zone. If no carrier gas is used, the high temperatures associated with the reactions zone, combined with the significant temperature gradients between the cold gas injection zone and the reaction zone will cause the gases to concentrate in the inlet of the pipe, forming a thick black liquid substance. By using a carrier gas, formation of this liquid is minimized. Titanium tetra isopropoxide ( $\text{Ti}(\text{OC}_3\text{H}_7)_4$ , Aldrich, %97), used as a precursor.



**Figure 3. Main Titanium Tetraisopropoxide (TTIP) Precursor**

Argon gas flow at 100 SCCM and ammonia gas flow at 200 SCCM are directed into the chamber and the furnace temperature is increased to 600 °C, once the experiment reaches 30 minutes the flow of gases are cut and the furnace is cooled down to room temperature, where argon gas at the flow of 100 SCCM is reintroduced into the chamber. The next stage is sample analysis using EDX and FESEM.

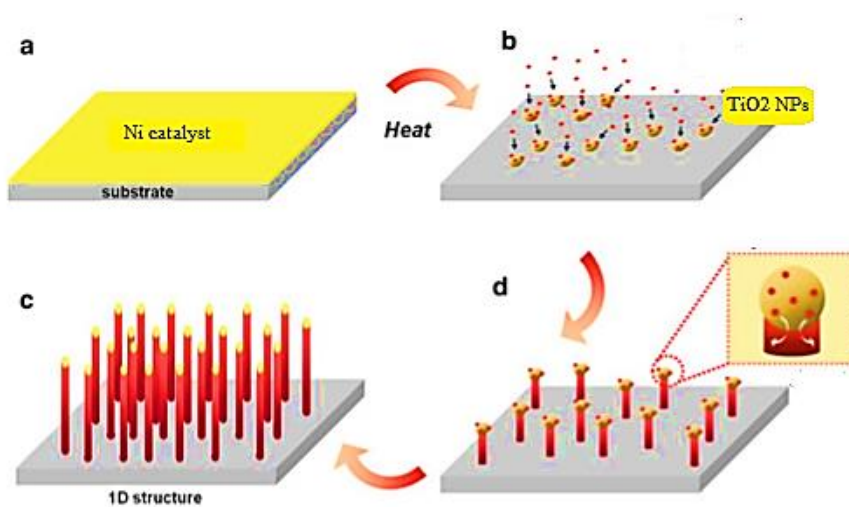


**Figure 4. Schematic of Titanium Dioxide 1D Nanoparticles Growth Using the TCVD System**

Table 1 lists the conditions and parameters for titanium dioxide nanoparticles synthesis using cobalt catalyst at 600 °C for different precursors and feed gases.

**Table 2. Conditions for Titanium Dioxide Nanoparticles Synthesis Using Various Gases**

Feeding gas	precursor	Catalyst	time (min)	Temperature (°C)

Ar	TTIP	Co	30	600
Ar + NH <sub>3</sub>	TTIP			
Ar	EtOH+TTIP			
Ar + NH <sub>3</sub>	EtOH+TTIP			

### 3. Results

#### 3.1. Rutherford Backscattering Spectrometry (RBS) Analysis

It is the prevalent characterization method for thin films, which uses high energy (order of several hundred mega eV) light ionic beams. Such beams are capable of penetrating thousands of angstroms or even several microns into the depth of the layers or the strata/substrate combination. These beams cause mild sputtering of the surface atoms and in return lose their incoming ions energy through ionization and excitation of the target atoms electrons. These electronic clashes are so high in number that the overall energy loss is almost always proportional to material depth.

One can extract information on the thickness and elemental composition of the layers through energy loss analysis of the reflecting ions.

This analysis was performed in the Atomic Energy Organization of Iran Research Institute on a U.S. made High Voltage Engineering Corp device. The integral condition for this method is for the sample to be in solid phase. In order to prepare the samples, the surface is grinded with sandpaper before being polished. Layer deposition period is 2.5 minutes and the cobalt catalyst thickness is 6.57 nm.

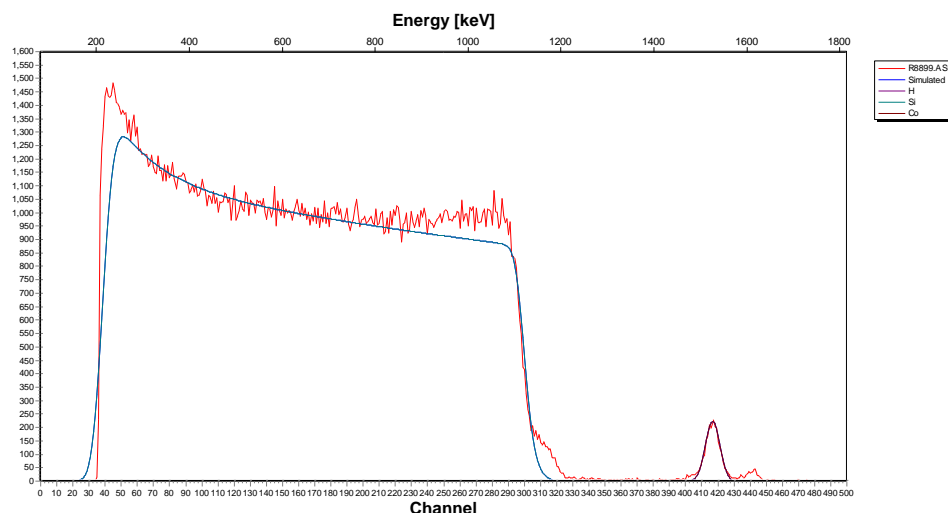


Figure 5. RBS Analysis for Cobalt Catalyst

Table 3. Cobalt Element Thickness on the Substrate

thickness	catalyst type
6.57 nm	Co

### 3.2. Atomic Force Microscopy (AFM) Analysis Results

The AFM is a powerful surface imaging method in the nanometer and micrometer range. Layer topography and surface roughness can be determined using this device. In order to determine the extent of surface unevenness on the samples, the initial sample and the radiation-subjected surface are studied. Figures below (Figures 6,7) display the AFM imagery. Roughness RMS measurement analysis from the AFM images gives an indication of surface unevenness. Roughness RMS measurement is performed using the equation below.

$$R_q = \sqrt{\frac{\sum(Z_i - Z_{avg})^2}{N}}$$

Roughness measurement equation

Where  $R_q$  is the surface roughness for the selected region,  $Z_i$  is the height of any given point,  $Z_{avg}$  is average height in selected region and  $N$  is the number of heightened points in the region[50].

#### 3.2.1. Pre-etching

Cobalt catalyst

Using this analysis, the structure and surface roughness on the cobalt catalyst are determined in the nanometer scale and the following results are produced. Figure 6 shows the results of the AFM as well as the average surface roughness which corresponds to 0.47 nanometers (nm).

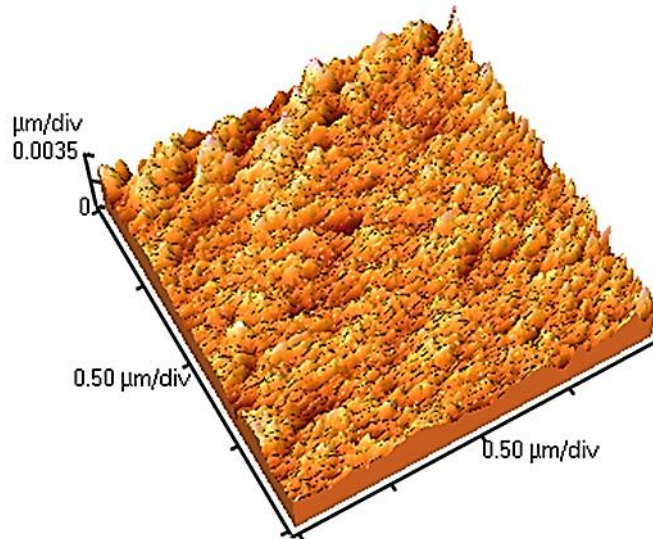


Figure 6. 3D geometric Structure of Cobalt Catalyst Using AFM

#### 3.2.2. Post-etching

Cobalt catalyst

Figure 7 shows AFM diagrams for the cobalt catalyst with an average roughness corresponding to 4.1 nm.



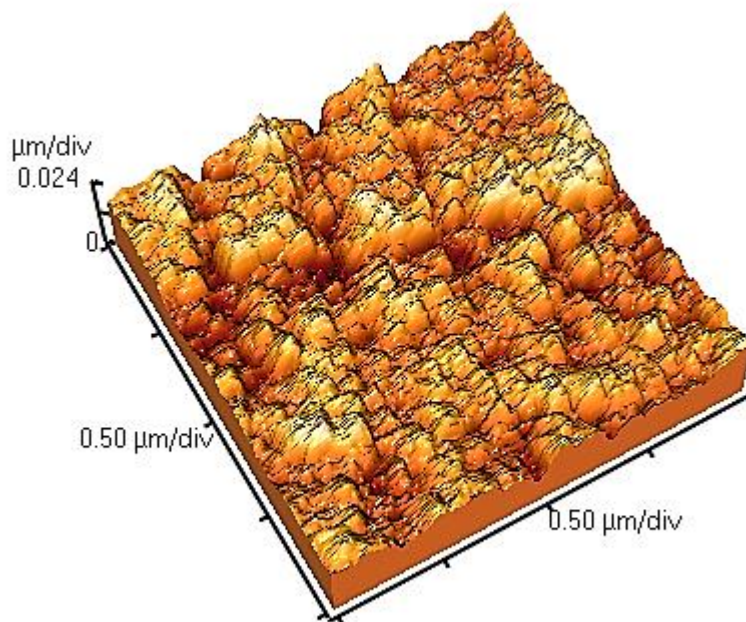


**Figure 7. Cobalt Catalyst Structure Direct Imagery Using AFM**

### **3.3. Field Emission Scanning Electron Microscope (FESEM) Analysis**

FESEM imagery of the synthesized samples are used for morphology analysis and determination of nanoparticle dimensions. Figures 8 a, b show titanium dioxide nanoparticles grown on cobalt catalyst bedding using titanium tetraisopropoxide as precursor; Figure 8.a shows argon as feed gas at 100 SCCM flow and Figure 8.b shows ammonia as feed gas at 200 SCCM flow where the resulting nanoparticle diameters on the catalyst are 22.92 and 19.83 nanometers respectively.

Ethanol is added to the nanoparticle growth precursor in the next stage, inserting different feed gases of argon at 100 SCCM (Figure 8.c) and ammonia and argon at 200 SCCM (Figure 8.d) resulting in nanoparticle dimensions of 26.4 nm and 48.7 nm, respectively.

### **3.4. Energy Dispersive X-ray Spectroscopy (EDX) Analysis**

Energy dispersive X-ray spectroscopy is used to analyze the elemental structures available in the sample. EDX point analysis of the samples is shown in Figures 9.a and 9.b where available elements within the samples are listed by weight and atomic percentages.

The sample which has been deposited by ammonia feed gas shows 48.59% titanium weight percentage, whereas the sample synthesized without ammonia feed gas shows a value of 42.37%, implying that ammonia gas has a significant effect on Ti levels, directly influencing its percentage.



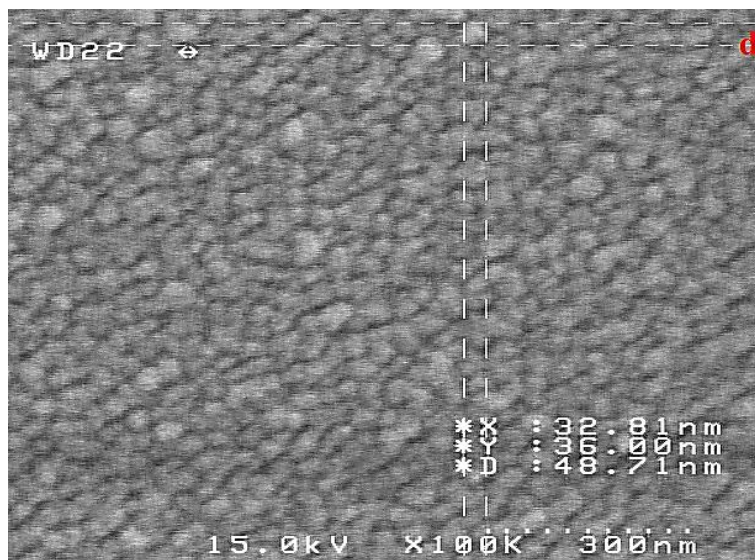


Figure 8. Cobalt Catalyst, Titanium Dioxide Nanostructure FESEM Imagery.

a) TTIP-Ar, b) TTIP-Ar- NH3, c) EtOH+TTIP-Ar, d) EtOH+TTIP-Ar-NH3

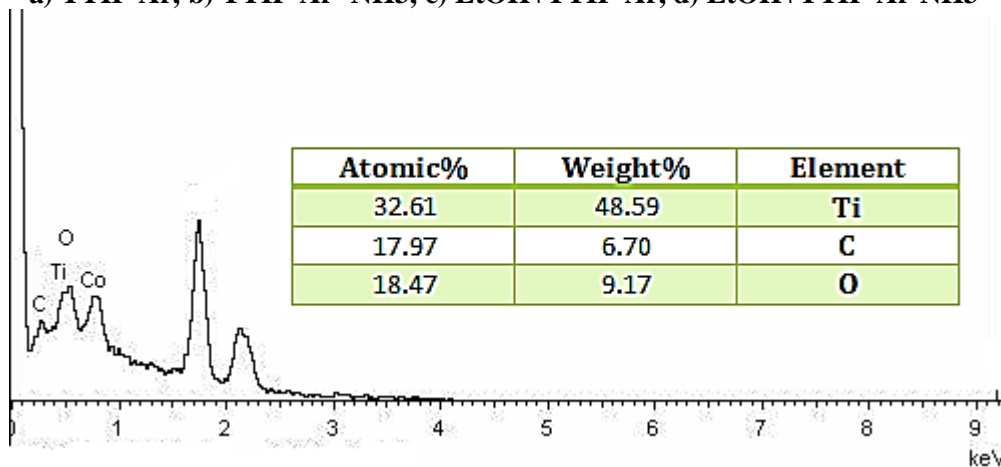


Figure 9.a. EDX analysis of Cobalt catalyst, titanium dioxide nanostructure with TTIP precursor, feed gas Ar+NH3

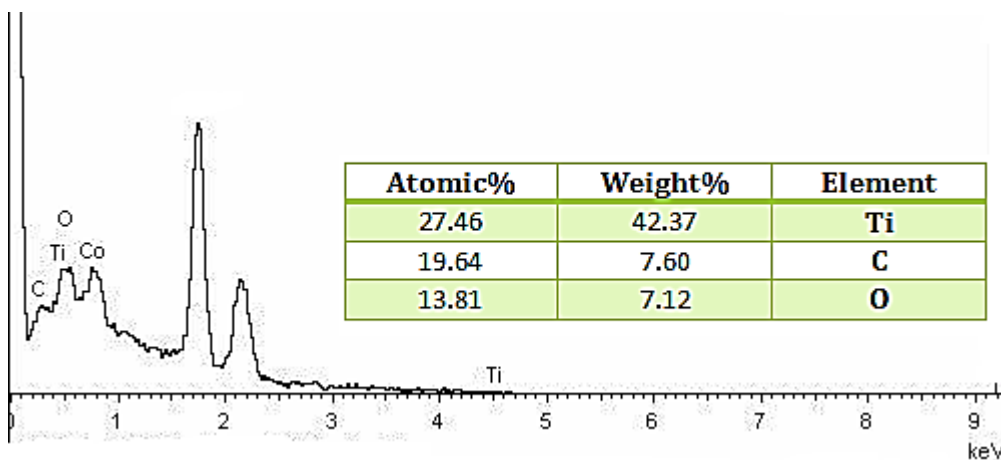


Figure 9.b. EDX Analysis of Cobalt Catalyst, Titanium Dioxide Nanostructure with TTIP Precursor, Feed Gas Ar

Weight percent diagrams for the elements of titanium, carbon and oxygen are shown under different conditions and various feed gases on the cobalt catalyst with titanium tetraisopropoxide precursor in Figure 10.

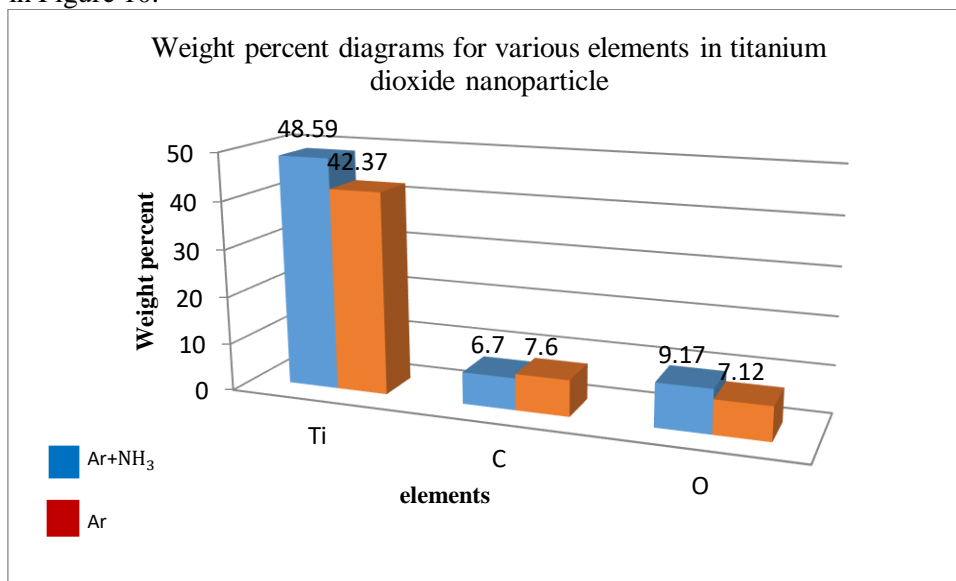


Figure 10. Weight Percent Diagrams for Various Elements in Titanium Dioxide Nanoparticle

#### 4. Conclusions

Nanotechnology is regarded today as a key technology in numerous fields worldwide. Considering its potential for removal of environmental pollution, purification and emission control, nanotechnology can be regarded as a green technology and an effective tool for achieving sustainable development. Presenting the highest surface to volume ratios, nanoscales play a decisive part in the removal of various pollutants. As such, nanotechnology with its unique capabilities can be considered as a viable option for polluted and sewage water recuperation as well as water desalination. The present work investigates the applications of nanotechnology in water purification and desalination, as well as the synthesis of these nanoparticles.

The effects of precursor concentrations, feed gas and synthesis method using TCVD is studied. TiO<sub>2</sub> nanoparticles were successfully synthesized as confirmed from FESEM and EDX. The precursor is inserted into the furnace at 600°C and the effect of ethanol injection into the precursor on nanoparticle crystal dimensions is studied and analyzed. AFM analyses of the cobalt catalyst surface are performed, before and after etching and EDX and FESEM analyses are also performed on the resulting nanoparticles. The results indicate ethanol addition to the system to cause the nanoparticle dimensions to increase, EDX analysis results indicate high titanium purity in these nanoparticles.

It can be concluded that the application of TiO<sub>2</sub> nanoparticles in membranes, due to its photocatalytic properties, can improve membrane performance factors such as water flux, salt excretion and clogging, rendering this material as the best option for membrane applications. Further research to characterize the amount, thickness and kinetics of the coating is necessary.

#### Acknowledgment +

I would like to convey my deep sense of thanks to the faculty of Physics Department, physics College, Islamic Azad University Tehran for their support in carrying out this research work.

#### References

- [1] E.J. Sullivan Graham, Noel. Baktian, et all , Energy for Water and Desalination, [Current Sustainable/Renewable Energy Reports](#), (2017)109–116.

- [2] A. Bouarioua, M. Zerdaoui, Photocatalytic activities of TiO<sub>2</sub> layers immobilized on glass substrates by dip-coating technique towards the decolorization of methyl orange as a model organic pollutant, *J. Environ. Chem. Eng.* 5 (2017) 1565–1574.
- [3] M. Nasirian, M. Mehrvar, Modification of TiO<sub>2</sub> to enhance photocatalytic degradation of organics in aqueous solutions, *J. Environ. Chem. Eng.* 4 (2016) 4072–4082.
- [4] N. Aman, N.N. Das, T. Mishra, Effect of N-doping on visible light activity of TiO<sub>2</sub>-SiO<sub>2</sub> mixed oxide photocatalysts, *J. Environ. Chem. Eng.* 4 (2016) 191–196.
- [5] M. Abdennouri, A. Elhalil, M. Farnane, H. Tounsadi, F.Z. Mahjoubi, R. Elmoubarki, M. Sadiq, L. Khamar, A. Galadi, M. Baâlala, M. Bensitel, Y. El Hafiane, A. Smith, N. Barka, Photocatalytic degradation of 2,4-D and 2,4-DP herbicides on Pt/TiO<sub>2</sub> nanoparticles, *J. Saudi Chem. Soc.* 19 (2015) 485–493.
- [6] J.Chen, S.C.Kou, C.S. Poon, Photocatalytic cement-based materials: comparison of nitrogen oxides and toluene removal potentials and evaluation of self-cleaning performance. *Build. Environ.*, 46(2011),1827–1833.
- [7] M.M.Ballari, M.Hunger, G.Hüsken, H. Brouwers, NO<sub>x</sub> photocatalytic degradation employing concrete pavement containing titanium dioxide. *Appl. Catal. B Environ.*, 95 (2010), 245–254.
- [8] G.Hüsken, M.Hunger, H. Brouwers, Experimental study of photocatalytic concrete products for air purification. *Build. Environ.* 44(2009), 2463–2474.
- [9] C.J. Vörösmarty, A.Y. Hoekstra, S.E. Bunn, D. Conway, J. Gupta, Fresh water goes global, *Science* 349 (2015) ,478–479.
- [10] J. Eliasson, The rising pressure of global water shortages, *Nature* 517 (2015) 6.
- [11] I.K. Konstantinou, T.A. Albanis, TiO<sub>2</sub>-assisted photocatalytic degradation of azo dyes in aqueous solution: kinetic and mechanistic investigations, *Appl. Catal. B-Environ.* 49 (2004) 1–14.
- [12] H. Lin, W. Gao, F. Meng, B.-Q. Liao, K.-T. Leung, L. Zhao, J. Chen, H. Hong, Membrane bioreactors for industrial wastewater treatment: a critical review, *Crit. Rev. Environ. Sci. Technol.* 42 (2012) 677–740.
- [13] X. Wang, V.W.C. Chang, C.Y. Tang, Osmotic membrane bioreactor (OMBR) technology for wastewater treatment and reclamation: Advances, challenges, and prospects for the future, *J. Membr. Sci.* 504 (2016) 113–132.
- [14] Y. Long, X. You, Y. Chen, H. Hong, B.-Q. Liao, H. Lin, Filtration behaviors and fouling mechanisms of ultrafiltration process with polyacrylamide flocculation for water treatment, *Sci. Total Environ.* 703 (2020) 135540.
- [15] Z. Wang, J. Ma, C.Y. Tang, K. Kimura, Q. Wang, X. Han, Membrane cleaning in membrane bioreactors: a review, *J. Membr. Sci.* 468 (2014) 276–307.
- [16] J. Chen, M. Zhang, F. Li, L. Qian, H. Lin, L. Yang, X. Wu, X. Zhou, Y. He, B.-Q. Liao, Membrane fouling in a membrane bioreactor: High filtration resistance of gel layer and its underlying mechanism, *Water Res.* 102 (2016) 82–89.
- [17] J. Teng, Y. Chen, G. Ma, H. Hong, T. Sun, B.-Q. Liao, H. Lin, Membrane fouling by alginate in polyaluminum chloride (PACl) coagulation/microfiltration process: Molecular insights, *Sep. Purif. Technol.* 236 (2020) 116294.
- [18] S. Hong, M. Elimelech, Chemical and physical aspects of natural organic matter (NOM) fouling of nanofiltration membranes, *J. Membr. Sci.* 132 (1997) 159–181.
- [19] M. Zhang, H. Hong, H. Lin, L. Shen, H. Yu, G. Ma, J. Chen, B.-Q. Liao, Mechanistic insights into alginate fouling caused by calcium ions based on terahertz time-domain spectra analyses and DFT calculations, *Water Res.* 129 (2018) 337–346.
- [20] Y. Chen, J. Teng, B.-Q. Liao, R. Li, H. Lin, Molecular insights into the impacts of iron(III) ions on membrane fouling by alginate, *Chemosphere* 242 (2020) 125232.
- [21] H. Lin, M. Zhang, F. Wang, F. Meng, B.-Q. Liao, H. Hong, J. Chen, W. Gao, A critical review of extracellular polymeric substances (EPSs) in membrane bioreactors: Characteristics, roles in membrane fouling and control strategies, *J. Membr. Sci.* 460 (2014) 110–125.
- [22] F. Meng, S. Zhang, Y. Oh, Z. Zhou, H.-S. Shin, S.-R. Chae, Fouling in membrane bioreactors: An updated review, *Water Res.* 114 (2017) 151–180.

- [23] J. Teng, L. Shen, Y. Xu, Y. Chen, X.-L. Wu, Y. He, J. Chen, H. Lin, Effects of molecular weight distribution of soluble microbial products (SMPs) on membrane fouling in a membrane bioreactor (MBR): Novel mechanistic insights, *Chemosphere* 248 (2020) 126013.
- [24] F. Xu, M. Wei, X. Zhang, Y. Song, W. Zhou, Y. Wang, How Pore Hydrophilicity Influences Water Permeability?, *Research* 2019 (2019) 10.
- [25] Y. Xu, D. Guo, T. Li, Y. Xiao, L. Shen, R. Li, Y. Jiao, H. Lin, Manipulating the mussel-inspired co-deposition of tannic acid and amine for fabrication of nanofiltration membranes with an enhanced separation performance, *J. Colloid Interf. Sci.* 565 (2020) 23–34.
- [26] L. Rao, J. Tang, S. Hu, L. Shen, Y. Xu, R. Li, H. Lin, Inkjet printing assisted electroless Ni plating to fabricate nickel coated polypropylene membrane with improved performance, *J. Colloid Interf. Sci.* 565 (2020) 546–554.
- [27] F. Chen, X. Shi, X. Chen, W. Chen, An iron (II) phthalocyanine/poly(vinylidene fluoride) composite membrane with antifouling property and catalytic selfcleaning function for high-efficiency oil/water separation, *J. Membr. Sci.* 552 (2018) 295–304.
- [28] D. Guo, Y. Xiao, T. Li, Q. Zhou, L. Shen, R. Li, Y. Xu, H. Lin, Fabrication of highperformance composite nanofiltration membranes for dye wastewater treatment: mussel-inspired layer-by-layer self-assembly, *J. Colloid Interf. Sci.* 560 (2020) 273–283.
- [29] L. Shen, Y. Zhang, W. Yu, R. Li, M. Wang, Q. Gao, J. Li, H. Lin, Fabrication of hydrophilic and antibacterial poly(vinylidene fluoride) based separation membranes by a novel strategy combining radiation grafting of poly(acrylic acid) (PAA) and electroless nickel plating, *J. Colloid Interf. Sci.* 543 (2019) 64–75.
- [30] Q. Qin, Z.C. Hou, X.F. Lu, X.K. Bian, L.F. Chen, L.G. Shen, S. Wang, Microfiltration membranes prepared from poly(N-vinyl-2-pyrrolidone) grafted poly(vinylidene fluoride) synthesized by simultaneous irradiation, *J. Membr. Sci.* 427 (2013) 303–310.
- [31] A. Abdel-Karim, T.A. Gad-Allah, A.S. El-Kalliny, S.I.A. Ahmed, E.R. Souaya, M.I. Badawy, M. Ulbricht, Fabrication of modified polyethersulfone membranes for wastewater treatment by submerged membrane bioreactor, *Sep. Purif. Technol.* 175 (2017) 36–46.
- [32] F.F. Ghiggi, L.D. Pollo, N.S.M. Cardozo, I.C. Tessaro, Preparation and characterization of polyethersulfone/N-phthaloyl-chitosan ultrafiltration membrane with antifouling property, *Eur. Polym. J.* 92 (2017) 61–70.
- [33] J. Garcia-Ivars, M.-I. Alcaina-Miranda, M.-I. Iborra-Clar, J.-A. Mendoza-Roca, L. Pastor-Alcañiz, Enhancement in hydrophilicity of different polymer phaseinversion ultrafiltration membranes by introducing PEG/Al<sub>2</sub>O<sub>3</sub> nanoparticles, *Sep. Purif. Technol.* 128 (2014) 45–57.
- [34] N. Li, Y. Tian, J. Zhang, Z. Sun, J. Zhao, J. Zhang, W. Zuo, Precisely-controlled modification of PVDF membranes with 3D TiO<sub>2</sub>/ZnO nanolayer: enhanced anti-fouling performance by changing hydrophilicity and photocatalysis under visible light irradiation, *J. Membr. Sci.* 528 (2017) 359–368.
- [35] J. Lin, W. Ye, K. Zhong, J. Shen, N. Jullok, A. Sotto, B. Van der Bruggen, Enhancement of polyethersulfone (PES) membrane doped by monodisperse Stöber silica for water treatment, *Chem. Eng. Process.* 107 (2016) 194–205.
- [36] A.L. Ahmad, A.A. Abdulkarim, Z.M.H. Mohd Shafie, B.S. Ooi, Fouling evaluation of PES/ZnO mixed matrix hollow fiber membrane, *Desalination* 403 (2017) 53–63.
- [37] W. Yu, Y. Liu, L. Shen, Y. Xu, R. Li, T. Sun, H. Lin, Magnetic field assisted preparation of PES Ni@MWCNTs membrane with enhanced permeability and antifouling performance, *Chemosphere* 243 (2020) 125446.
- [38] N. Ghaemi, S.S. Madaeni, P. Daraei, H. Rajabi, S. Zinadini, A. Alizadeh, R. Heydari, M. Beygzadeh, S. Ghouzivad, Polyethersulfone membrane enhanced with iron oxide nanoparticles for copper removal from water: Application of new functionalized Fe<sub>3</sub>O<sub>4</sub> nanoparticles, *Chem. Eng. J.* 263 (2015) 101–112.
- [39] A. Ananth, G. Arthanareeswaran, A.F. Ismail, Y.S. Mok, T. Matsuura, Effect of bio-mediated route synthesized silver nanoparticles for modification of polyethersulfone membranes, *Colloids Surf. A* 451 (2014) 151–160.

- [40] A.Mills, S.K. A.Lee, web-based overview of semiconductor photochemistry-based current commercial applications. *J. Photochem. Photobiol. A Chem.* 152(2002), 233–247.
- [41] U.I.Gaya, A.H.Abdullah, Heterogeneous photocatalytic degradation of organic contaminants over titanium dioxide: A review of fundamentals, progress and problems. *J. Photochem. Photobiol. C Photochem. Rev.* 9(2008), 1–12.
- [42] S. Leong, A. Razmjou, K. Wang, K. Hapgood, X. Zhang, H. Wang, TiO<sub>2</sub> based photocatalytic membranes: a review, *J. Membr. Sci.* 472 (2014) 167–184.
- [43] E. Bet-moushoul, Y. Mansourpanah, K. Farhadi, M. Tabatabaei, TiO<sub>2</sub> nanocomposite based polymeric membranes: A review on performance improvement for various applications in chemical engineering processes, *Chem. Eng. J.* 283 (2016) 29–46.
- [44] E.S. Dz`unuzovic´, J.V. Dz`unuzovic´, A.D. Marinkovic´, M.T. Marinovic´-Cincovic´, K.B. Jeremic´, J.M. Nedeljkovic´, Influence of surface modified TiO<sub>2</sub> nanoparticles by gallates on the properties of PMMA/TiO<sub>2</sub> nanocomposites, *Eur. Polym. J.* 48 (2012) 1385–1393.
- [45] H. Tong, S. Ouyang, Y. Bi, N. Umezawa, M. Oshikiri, J. Ye, Nano-photocatalytic materials: possibilities and challenges, *Adv. Mater.* 24 (2012) 229–251.
- [46] T. Sirinpong, W. Youravong, D. Tirawat, W.J. Lau, G.S. Lai, A.F. Ismail, Synthesis and characterization of thin film composite membranes made of PSF-TiO<sub>2</sub>/GO nanocomposite substrate for forward osmosis applications, *Arabian J. Chem.* 11 (2018) 1144–1153.
- [47] P. Daraei, S.S. Madaeni, N. Ghaemi, M.A. Khadivi, B. Astinchap, R. Moradian, Fouling resistant mixed matrix polyethersulfone membranes blended with magnetic nanoparticles: Study of magnetic field induced casting, *Sep. Purif. Technol.* 109 (2013) 111–121.
- [48] Z. Xu, T. Wu, J. Shi, W. Wang, K. Teng, X. Qian, M. Shan, H. Deng, X. Tian, C. Li, F. Li, Manipulating Migration Behavior of Magnetic Graphene Oxide via Magnetic Field Induced Casting and Phase Separation toward High-Performance Hybrid Ultrafiltration Membranes, *ACS Appl. Mater. Interfaces* 8 (2016) 18418–18429.
- [49] Y. Huang, C.-F. Xiao, Q.-L. Huang, H.-L. Liu, J.-Q. Hao, L. Song, Magnetic field induced orderly arrangement of Fe<sub>3</sub>O<sub>4</sub>/GO composite particles for preparation of Fe<sub>3</sub>O<sub>4</sub>/GO/PVDF membrane, *J. Membr. Sci.* 548 (2018) 184–193.
- [50] M. Hollaus, M. Milenković, N. Pfeifer, A Review of Surface Roughness Concepts, Indices and Applications, *J. Alpine space*. Project number 2-3-2-FR (2014).